I&EC research
Industrial & Engineering Chemistry Research

Article

Evaluation thermophysical properties of functionalized imidazolium thiocyanate based ionic liquids

Girma Gonfa, Mohamad Azmi Bustam, Nawshad Muhammad, and Amir Sada Khan

Ind. Eng. Chem. Res., **Just Accepted Manuscript** • DOI: 10.1021/acs.iecr.5b03707 • Publication Date (Web): 19 Nov 2015

ACS Publications

Industrial & Engineering Chemistry Research is published by the American Chemical Society. 1155 Sixteenth Street N.W., Washington, DC 20036

Evaluation thermophysical properties of functionalized imidazolium thiocyanate based ionic liquids

Girma Gonfa[*†], *Mohamad Azmi Bustam*[†], *Nawshad Muhammad*[§], *Amir Sada Khan*[†]

[†]Chemical Engineering Department, Universiti Teknologi PETRONAS, 31750 Tronoh, Perak, Malaysia.

[§]Interdisciplinary Research Center in Biomedical Materials, COMSATS Institute of Information Technology, Lahore, Pakistan.

ABSTRACT

New cyano-based ionic liquids with thiocyanate anion, and nitrile, ally, benzyl and hydroxyl functionalized imidazolium cations were prepared and some of their important thermophysical properties were measured. Properties such as density, viscosity and refractive index were measured over various temperature ranges. From the experimental density values, the molecular volume, standard molar entropy, lattice energy and thermal expansion coefficient of the ionic liquids were calculated. The thermal stability of the ionic liquids was investigated using thermogravimetric analysis. The effects of functionalized imidazolium side chains on the thermophysical properties of the ionic liquids were investigated. Density functional theory (DFT) calculations were performed to study the effect of the structural variation of the imidazolium cation on properties of the ionic liquids.

1. INTRODUCTION

Cyano-based ionic liquids (ILs) are attracting considerable attention for industrial applications because they present lower melting points and viscosities compared to most of other ILs. [1, 2] Cyano-based ILs contain one or more cyano (CN) group in their structural moieties. The high electronegativity, stable triple bond and delocalized charges of the cyano group offered them very unique properties and applications. Initially, the cyano-based ILs were prepared, characterized and mainly used for electrochemical applications due to their high conductivity, high fluidity and low melting point.[2-6] Recently, these ILs have been used for dye-sensitized solar cells, [7, 8] separation of aromatic from aliphatic hydrocarbons, [1, 9, 10] gas separation [11] and bioseparation[12] and biomass treatment. [13] Consequently, some cyano-based ILs were synthesized and their thermophysical properties in their pure form and mixture with other solvents were reported.[14-23] However, most of the studied ILs are based on 1-butyl-3-methylimidazolium and 1-ethyl-3-methylimidazolium cations with cyano-based anions, mainly dicyanamide and thiocyanate. Only, few works were reported for ILs with nitrile functionalized imidazolium alkyl side- chain and cyano-based anions.[23] In our previous work [24], we reported the effects of nitrile, allyl, benzyl and hydroxyl functional groups on the thermophysical properties of four ILs based on dual functionalized imidazolium cations and chloride anion. To the best of our knowledge, the thermophysical properties of ILs with dual functionalized imidazolium alkyl side-chain and cyano based anions have not been studied yet.

The current work presents the synthesis and some of the important thermophysical properties of five cyano based-ILs with thiocyanate anion, and nitrile, hydroxyl, benzyl and allyl functionalized imidazolium cations. The effects of the functional groups on the thermophysical properties of the ILs were presented. Density functional theory (DFT) calculations were

performed to support the proposed arguments applied to explain the effects of the functional groups on the properties of the ILs. The studied ILs are, namely, 1-butyl-3-methylimidazolium thiocyanate ([Bmim][SCN]), 3-(3-butyl-1H-imidazol-3-ium-1-yl)propanenitrile thiocyanate ([C_2CNBim][SCN]), 3-(3-allyl-1H-imidazol-3-ium-1-yl)propanenitrile thiocyanate ([C_2CNAim][SCN]), 3-(3-benzyl-1H-imidazol-3-ium-1-yl)propanenitrile thiocyanate ([C_2CNBzim][SCN]), 3-[3-(2-hydroxyethyl)-1H-imidazol-3-ium-1-yl]propanenitrile thiocyanate ([C_2CNHeim][SCN]). The structure of the studied ILs are depicted in Figure 1.

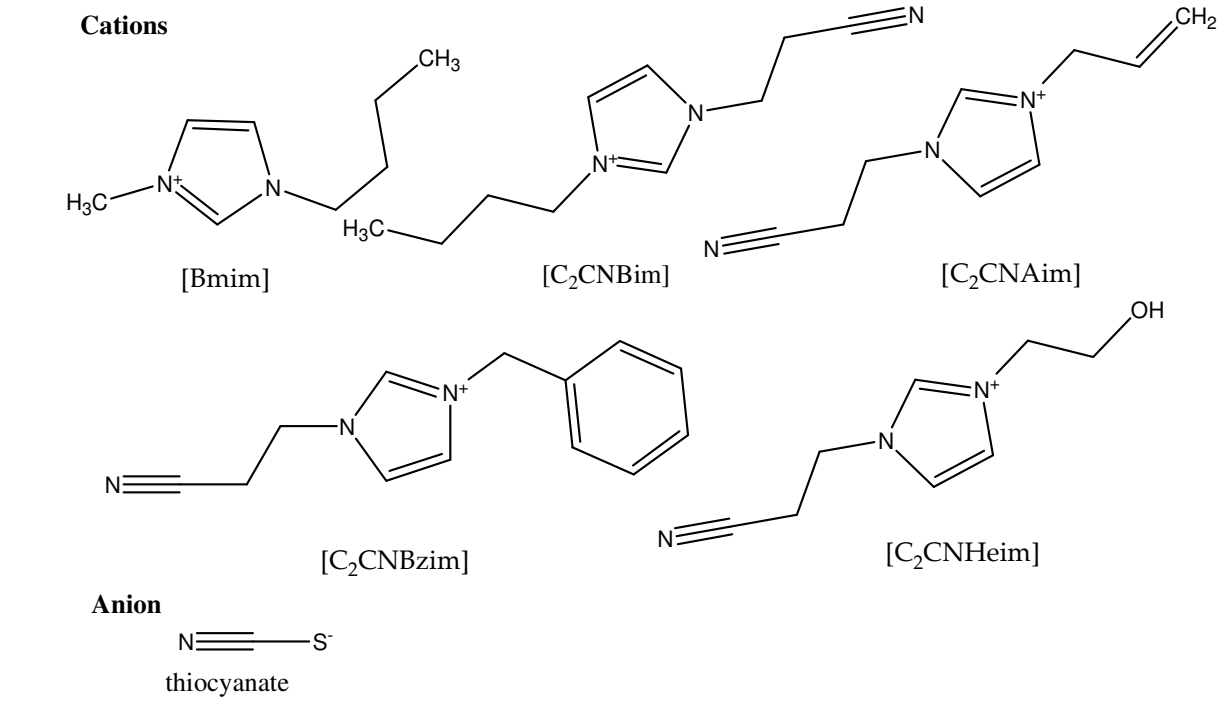

Figure 1. Structure of the studied ILs.

2. EXPERIMENTAL SECTION

2.1. Materials

The ionic liquids were synthesized using analytical grade chemicals without further purifications. The starting materials are: imidazole (Aldrich, 99%), 1-methylimidazole (Merck, 99%), acrylonitrile (Aldrich, 99%), 2-chloroethanol (Merck, 99.8%), benzyl chloride (Merck, 99%),

allyl chloride (Aldrich, 98%), 1-chlorobutane (Merck, 99%), sodium thiocyanate (Sigma-Aldrich, 98%), methanol (anhydrous, Aldrich, 99.8%), acetone (Aldrich, 99.8%), 1-chlorobutane (Aldrich, 99.5% and ethyl acetate (anhydrous, Aldrich, 99.8%). 1-butyl-3-methylimidazolium chloride (98%) was obtained from Sigma-Aldrich.

2.2. Preparation of ionic liquids

[Bmim][SCN] was prepared by metathesis reaction of 1-butyl-3-methylimidazolium chloride ([Bmim]Cl) with sodium thiocyanate as described in the literature. [20] The synthesis procedure adopted for the other four ILs consists of four steps: incorporation of nitrile group into the imidazolium cation through Michael addition reaction, preparation of their respective chloride based ILs and further exchange of chloride with thiocyanate anion. The chloride based ILs, namely, 3-(3-butyl-1H-imidazol-3-ium-1-yl)propanenitrile chloride ([C_2CNBim]Cl), 3-(3-allyl-1H-imidazol-3-ium-1-yl)propanenitrile chloride ([C_2CNAim]Cl), 3-(3-benzyl-1H-imidazol-3-ium-1-yl)propanenitrile chloride ([C_2CNBzim]Cl) and 3-[3-(2-hydroxyethyl)-1H-imidazol-3-ium-1-yl]propanenitrile chloride ([C_2CNHeim]Cl) were prepared using the procedures reported in our previous work. [24] Subsequently, the desired ILs, named, 3-(3-butyl-1H-imidazol-3-ium-1-yl)propanenitrile thiocyanate, 3-(3-allyl-1H-imidazol-3-ium-1-yl)propanenitrile thiocyanate, 3-(3-benzyl-1H-imidazol-3-ium-1-yl)propanenitrile thiocyanate and 3-[3-(2-hydroxyethyl)-1H-imidazol-3-ium-1-yl]propanenitrile thiocyanate were prepared from their corresponding chloride based ILs through metathesis reaction with sodium thiocyanate. Bruker Avance 500 spectrometer was used to record the ^{1}H and ^{13}C NMR spectra. The elemental analyses were performed using CHNS-932 (LECO instruments). The ^{1}HNMR and ^{13}CNMR and elemental analysis of the ILs are given below.

1-butyl-3-methylimidazolium thiocyanate. ^{1}H NMR ($CDCl_3$): δ (ppm) = 0.89 (3H, t), 1.31 (2H, m), 1.86 (2H, m), 4.12 (3H, s), 4.28 (2H, t), 7.42 (1H, m), 7.56 (1H, m), 10.55 (1H, s). ^{13}CNMR ($CDCl_3$): δ (ppm) = 13.5, 19.9, 32.1, 35.8, 51.3, 122.3, 126.7, 134.5, and 138.1. Elemental analysis: C (54.7 %), H (7.8 %), N (21.3 %), S (16.2 %). Theoretical: C (54.8 %), H (7.7 %), N (21.3 %), S (16.2 %).

3-(3-butyl-1H-imidazol-3-ium-1-yl)propanenitrile thiocyanate. ^{1}H NMR (DMSO-d_6): δ (ppm) = 0.96 (3H, t), 1.31 (2H, m), 1.81 (2H, m), 3.07 (2H, t), 4.18 (2H, t), 4.47 (2H, t), 7.66 (1H, s). ^{13}C NMR (DMSO-d_6): δ (ppm) = 14.1, 18.3, 21.7, 29.4, 48.5, 50.7, 120.5, 121.9, 124.3, and 134.5. Elemental analysis: C (55.9 %), H (6.8 %), N (23.7 %), S (13.5 %). Theoretical: C (55.9 %), H (6.7 %), N (23.6 %), S (13.6 %).

3-(3-allyl-1H-imidazol-3-ium-1-yl)propanenitrile thiocyanate. ^{1}H NMR (DMSO-d_6): δ = 3.20 (2H, t), 4.55 (2H, t), 4.91 (2H, d), 5.35 (2H, d), 6.15 (1H, m), 7.75 (1H, s), 7.89 (1H, s), 9.15 (1H, s). ^{13}C NMR (DMSO-d_6): δ (ppm) = 18.2, 46.9, 54.1, 114.9, 118.5, 119.4, 121.7, 122.6, 125.8, 133.3. Elemental analysis: C (54.5 %), H (5.4 %), N (25.4 %), S (14.5 %). Theoretical: C (54.3 %), H (5.3 %), N (23.1 %), S (17.1 %).

3-(3-benzyl-1H-imidazol-3-ium-1-yl)propanenitrile thiocyanate. ^{1}H NMR (DMSO-d_6): δ = 3.25 (2H, t), 4.59 (2H, t), 5.45 (2H, s), 7.47 (5H, m), 7.91 (1H, s), 7.95(1H, s), 9.65 (1H, s). ^{13}C NMR (DMSO-d_6): δ (ppm) = 17.9, 47.2, 56.7, 118.3, 119.4, 121.9, 122.3, 124.5, 125.6, 129.1, 129.2, 130.1, 130.3, 138.6. Elemental analysis: C (62.2 %), H (5.2 %), N (20.7 %), S (11.8 %). Theoretical: C (62.3 %), H (5.0 %), N (21.1 %), S (11.4 %).

3-[3-(2-hydroxyethyl)-1H-imidazol-3-ium-1-yl]propanenitrile thiocyanate. ^{1}H NMR (DMSO-d_6): δ = 3.25 (2H, t), 3.75 (2H, t), 4.22 (2H, t), 5.37 (2H, d), 5.45 (1H, t), 7.91 (1H, s), 7.85 (1H, s), 9.45 (1H, s). ^{13}C NMR (DMSO-d_6): δ (ppm) = 17.5, 47.6, 54.1, 59.3, 118.7, 119.3, 121.5,

122.9, 124.9. Elemental analysis: C (48.2 %), H (5.3 %), N (24.9 %), S (14.3 %). Theoretical: C (47.8 %), H (5.7 %), N (24.7 %), S (14.8 %).

2.3. Properties measurements

Before measuring the properties, the ILs were rigorously purified using ethyl acetate and diethyl ether and dried in a vacuum oven at 80 °C for 48 h. The water contents were measured using coulometric Karl Fischer titrator (model DL39). The halide content was measured using ion chromatogram (Metrohm model 761 Compact IC). The water and chloride contents of the ILs are given in Table 1.

Table 1. Water and chloride contents of the ILs.

	[Bmim][SCN]	[C_2CNBim][SCN]	[C_2CNAim][SCN]	[C_2CNBzim][SCN]	[C_2CNeHim][SCN]
Water content (ppm)	257	305	283	318	353
Chloride content (ppm)	63	72	76	89	94

2.4. Thermal decomposition temperature

Perkin-Elmer, Pyris V-3.81 thermal gravimetric analyser (TGA) was used to investigate the short term thermal stability of the ILs in nitrogen atmosphere. Samples (4 mg) were placed in an aluminium pan under a nitrogen atmosphere at a heating rate of 10 K/min from 323 to 900 K. The temperature accuracy is better than ± 1 K. The onset temperature (T_{onset}), starting temperature (T_{start}), peak temperature (T_{peak}) and the temperature at which 10% of the sample decomposed ($T_{10\%}$) were obtained from TGA analyses.

2.5. Density and viscosity measurements

Density and viscosities were measured using the Anton Paar Viscometer (model SVM3000). Before measuring the densities and viscosities, the instrument were calibrated using ultrapure millipore quality water and validated with ILs of established properties. [24] The densities and viscosities were measured over a temperature range of (293.15 - 353.15) K and at atmospheric

pressure. The uncertainty of measurements are $u(T) = \pm 0.01$ K, $u(\eta) = \pm 0.32$ % and $u(\rho) = \pm 5\times10^{-6}$ g·cm^{-3} for temperature, viscosity and density, respectively. All the measurements were performed three times to obtain the average values.

2.6. Refractive index measurements

ATAGO programmable digital refractometer (RX-5000α) was used to measure the refractive indexes of the ILs. The refractometer was calibrated using pure organic solvents with known refractive index values and validated with ILs of known properties. [24] The uncertainty in measurement of this equipment is of the order of $\pm 4\times10^{-5}$. Temperature was controlled within ± 0.05 K. The refractive index values were measured in the temperature range of (298.15 to 333.15) K. At least three measurements were done at each temperature and their average values were reported.

2.7. Computational Methods

Density functional theory (DFT) calculations were performed to understand the effect of the structural variations of the imidazolium cation on the molecular properties of the ILs. Turbomole 6.2 software package [25] was used for the quantum calculations. First the structure of the cations and thiocyanate anion were separately optimized. Then, ion-paired structures, combining each cation and thiocyanate anion, were optimized to simulate the ILs. The geometry optimizations were performed using the dispersion corrected density functional theory (DFT-dsp) method, utilizing the Becke-Perdew-86 (BP86) functional [26, 27] with resolution of identity (RI) approximation and a triple-ξ valence polarized basis set (TZVP). [28, 29] Natural Bond Orbital (NBO) population analyses for the species were performed at the same level and basis set. The ideal screening charges on the molecular surface for the species were calculated using COSMOthermX programme (version C2.1) with BP_TZVP_C21_0111.ctd parameterization [30].

3. RESULTS AND DISCUSSION

3.1. Density

The densities measurements for [Bmim][SCN] as a function of temperature were compared with literature values. [16, 18, 22] The relative differences between our measurement and those reported by Sanchez et al.[16], Vakili-Nezhaad et al. [22] and Królikowska et al. [18] varies from (0.013 to 0.05)%, (0.003 to 0.025)% and (0.008 to 070)%, respectively. The literature values along with the relative differences are given in supplementary documents (Table S1). The comparison between our measurements and the literature data is included in supporting information (Figure S1). For [Bmim][SCN], our density measurements are in good agreement with literature data. The remaining four ILs are new synthesis and therefore impossible to compare with reported literature.

The densities (ρ) of the ILs in the temperature range of (293.15- 353.15) K and at atmospheric pressure are reported in Table 2. The density increases in the order of [Bmim][SCN] < [C_2CNBim][SCN] < [C_2CNAim][SCN] < [C_2CNBzim][SCN] < [C_2CNHeim][SCN]. Incorporation of the nitrile functional group in the imidazolium alkyl chain increases the density of the ILs. This can be observed from the densities of [Bmim][SCN] and [C_2CNBim][SCN] for which the density values increases at least by 4% when nitrile functional group is incorporated in the imidazolium alkyl side-chain. This could be due to the strong dipole moment of the nitrile functional group that may be responsible for the formation of a more ordered cation and anion structure in the ILs. [23]

Incorporation of additional functional groups such as allyl, benzyl and hydroxyl on the other side of imidazolium cation further increases the densities of the ILs. When allyl, benzyl and hydroxyl functional groups replaces the butyl alkyl chain of [C_2CNBim][SCN] the densities increase by

more than 8%, 9% and 12%, respectively. Incorporation of the allyl, benzyl or hydroxyl functional groups to the nitrile functionalized imidazolium cation might cause strong electrostatic interactions, π-π stacking and hydrogen bonding which could cause efficient high packing. The highest density of hydroxyl functionalized [C_2CNHeim][SCN] could be attributed to the strong hydrogen bond formation ability of O-H functional group in the imidazolium cation. [31] The same trend was observed for their chloride based counterparts. That is, for chloride based dual functionalized ILs the density increases in the order of [C_2CNBim]Cl < [C_2CNAim]Cl < [C_2CNBzim]Cl < [C_2CNHeim]Cl. [24] The effects of the nitrile, allyl, benzyl and hydroxyl function of the structural properties of the studied ILs are discussed in section 3.10.

Table 2. Experimental densities (ρ/g·cm^{-3}) for the ILs as a function of temperature at atmospheric pressure[a]

T/K	[Bmim] [SCN]	[C_2CNBim] [SCN]	[C_2CNAim] [SCN]	[C_2CNBzim] [SCN]	[C_2CNHeim] [SCN]
293.15	1.072621	1.122939	1.165158	1.177327	1.218135
298.15	1.069683	1.119816	1.162104	1.174043	1.216229
303.15	1.066753	1.116744	1.159058	1.170771	1.213261
308.15	1.063817	1.113648	1.156030	1.167527	1.210294
313.15	1.060881	1.110577	1.153018	1.164253	1.208371
318.15	1.057942	1.107467	1.150019	1.161080	1.205164
323.15	1.055014	1.104461	1.147042	1.157947	1.201980
328.15	1.052073	1.101497	1.144020	1.154824	1.198739
333.15	1.049138	1.098555	1.141113	1.151708	1.195619
338.15	1.046203	1.095618	1.138217	1.148612	1.192555
343.15	1.043268	1.092694	1.135320	1.145536	1.189488
348.15	1.040333	1.089780	1.132424	1.142486	1.186422
353.15	1.037398	1.086892	1.129537	1.139460	1.183352

[a]*Standard uncertainties u are u(T) = ± 0.01 K and u(ρ) = ± 5×10^{-6} g·cm^{-3}.*

The densities decrease linearly with increasing temperature as shown in Figure 2. The densities of the ILs were fitted by least square methods to the following linear equation:

$$\rho = A_0 + A_1 T \quad (1)$$

where, ρ denote the density of the ILs (g.cm^{-3}), T is temperature in Kelvin, and A_0 and A_1 are the correlation coefficients. The values of A_o and A_1 were estimated using least square method. The fitting parameters along with the correlation coefficient and standard deviations for equation (1) provided in supporting information (Table S2). The densities as a function of temperature were successfully fitted with the linear equation with a correlation coefficient $R^2 > 0.99$ and maximum standard deviation (SD) < 0.0005 for all the studied ILs. The *SD* values were calculated by applying the following expression:

$$SD = \left[\frac{\sum(Z_{exp} - Z_{cal})^2}{n}\right]^{1/2} \quad (2)$$

where, *SD, n,* Z_{cal} and Z_{exp} are the standard deviation, number of experimental points, calculated and experimental values, respectively.

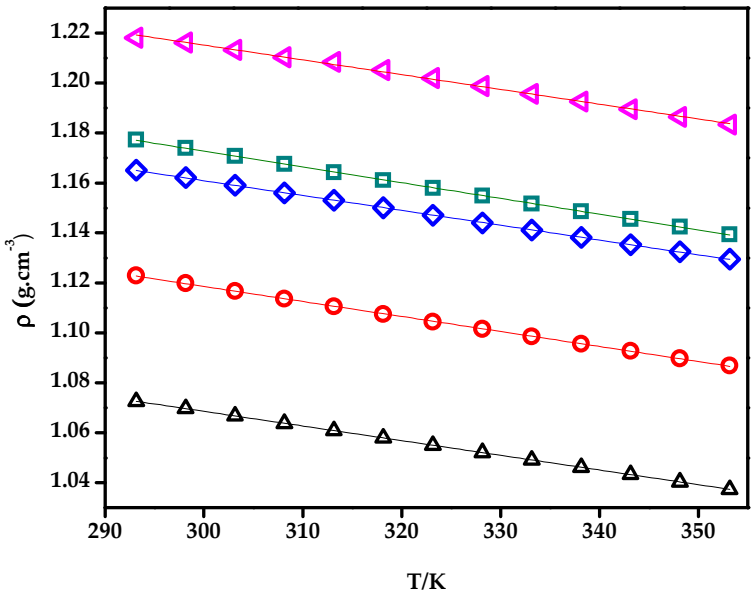

Figure 2. Temperature dependence for densities of the ILs. Δ, [Bmim][SCN]; ○, [C_2CNBim][SCN]; ◇, [C_2CNAim][SCN]; □, [C_2CNBzim] [SCN]; ◁, [C_2CNHeim][SCN].

The densities were used to calculate other important properties such as standard molar volume (V_m), molecular volume (V), standard entropy (S^0), crystal energy (U_{POT}), and isobaric thermal expansion coefficients (α_p) of the ILs.

3.2. Standard molar volume

Standard molar volume (V_m) is the volume occupied by one mole of a substance at standard temperature and pressure. The V_m values of the ILs were calculated at room temperature and atmospheric pressure using the following equation:

$$V_m = {}^{M}/_{\rho} \quad (3)$$

where, V_m is molar volume ($cm^3.mol^{-1}$), M is the molecular weight ($g.mol^{-1}$) and ρ is the density ($g.cm^{-3}$) at 298.15 K. The values of V_m calculated for the ILs are shown in Table 3. The V_m of the studied ILs follows the order of [Bmim][SCN] < [C_2CNHeim][SCN] < [C_2CNAim][SCN] < [C_2CNBzim][SCN] < [C_2CNBim][SCN].

The standard molar volumes of the present ILs are higher than their corresponding chloride based ILs reported in our previous work. [24] The V_m for [C_2CNBim]Cl, [C_2CNAim]Cl, [C_2CNBzim]Cl and [C_2CNHeim]Cl are 189.2, 168.8, 160.6 and 205.9 $cm^3.mol^{-1}$, respectively. The higher molar volume of the thiocyanate based could be due to the lower hydrogen basicity of thiocyanate anion compared with chloride anion. [32] Since the cation-anion interaction is low in ILs with anion of low hydrogen bond basicity, the thiocyanate based ILs have higher molar volume (less compacted) than chloride based ILs. The same conclusion can be reached from molecular volume of the ILs. The molecular volumes *(V)* of the ILs were calculated from molar volume and Avogadro's constant (N_A) using the following equation:

$$V = \frac{V_m}{N_A} \quad (4)$$

where, *NA* (Avogadro's constant) = 6.02245×10^{23} molecule per mol. The molecular volumes of the ILs were included in Table 3. The molecular volume of the ILs increase in the order of [Bmim][SCN] < [C_2CNHeim][SCN] < [C_2CNAim][SCN] < [C_2CNBzim][SCN] < [C_2CNBim][SCN].

Table 3**.** Molar volume (V_m), molecular volume (V), standard entropy (S^0) and crystal energy (U_{POT}) of the ILs at 298.15 K and at atmospheric pressure.

	[Bmim][SCN]	[C_2CNBim][SCN]	[C_2CNAim][SCN]	[C_2CNBzim][SCN]	[C_2CNHeim][SCN]
V_m ($cm^3.mol^{-1}$)	184.4	240.8	189.1	229.6	184.1
V (nm^3)	0.3063	0.3998	0.3139	0.3813	0.3057
$S°$ ($J.K^{-1}.mol^{-1}$)	65.3	109.1	68.1	98.6	65.1
U_{POT} ($kJ.mol^{-1}$)	451.8	422.3	449.0	427.3	452.1

3.3. Standard entropy

The values of standard entropy (S^0) were calculated from molecular volume using the relationship established by Glasser: [33]

$$S^0(J.K^{-1}mol^{-1}) \approx 1246.5\,V\,(nm^3) + 29.5 \quad (5)$$

where, V is the molecular volume of the ILs. The values of the standard entropy of the ILs are shown in Table 3. It can be observed that the standard entropy ($S^°$) follows the same trends as standard molar volume (V_m). Moreover, the value of the standard entropy of the studied ILs are higher that of their corresponding chloride based ILs. The standard entropy reported for [C_2CNBim]Cl, [C_2CNAim]Cl, [C_2CNBzim]Cl and [C_2CNHeim]Cl are 68.17, 56.96, 79.37, 53.17 $J.K^{-1}.mol^{-1}$.[24] The higher standard entropy values might be due to less interaction in the thiocyanate based ILs compared to their corresponding chloride based ILs.

3.4. Crystal energy

The crystal energy (U_{POT}) at 298.15 K were calculated using Glasser's theory: [33]

$$U_{POT}(kJ.mol^{-1}) = 1981.2\left(\rho/M\right)^{1/3} + 103.8 \quad (6)$$

where, ρ and M are the density (g.cm^{-3}) and molecular mass (g.mol^{-1}), respectively. The estimated crystal energies are given in Table 3. As expected the crystal energies of the studied ILs are much lower than those of inorganic fused salts. The crystal energy for cesium iodide, which has the lowest crystal energy among alkali-chlorides, is 613 kJ.mol^{-1}.[34] The crystal energies of the present ILs increases in the order of [C_2CNBim][SCN] < [C_2CNBzim][SCN] < [C_2CNAim][SCN] < [C_2CNHeim][SCN] ≈ [Bmim][SCN]. Moreover, the crystal energies of the ILs are lower than their corresponding chloride based ILs. The calculated crystal energies for [C_2CNBim]Cl, [C_2CNAim]Cl, [C_2CNBzim]Cl and [C_2CNHeim]Cl are 448.9, 462.3, 439.3, 468.2 kJ.mol^{-1}, respectively.[24] The lower crystal energy suggests the thiocyanate based ILs are less compacted than their equivalent chloride based ILs.

3.5. Isobaric Thermal Expansion Coefficient

The isobaric thermal expansion coefficients (α_p) of the ILs were calculated from experimental density values using equation (7):

$$\alpha_p = -\left(\frac{\partial \rho}{\partial T}\right)_P \quad (7)$$

where, ρ and T are the density and temperature, respectively. The values of isobaric thermal expansion coefficients as function of temperature are included in supporting information (Table S3). The variations of the thermal expansion coefficients with temperature are not significant for the present ILs. The isobaric expansion values are in the range of (4.85 to 5.55)×10^{-4} K^{-1} which is typical values for ILs. [18, 24] The thermal expansion coefficients of the ILs are noticeably lower than that of most molecular organic compounds, for instance for toluene, the values are in the range of (10.7 to 11.3)×10^{-4} K^{-1} [35]. Moreover, thermal expansion coefficients of the ILs are

greater than the thermal expansion coefficients of high temperature molten salt. For instance, *the* isobaric thermal expansion coefficients for NaCl and KCl at 1100 K are 3.094×10^{-4} and 3.632×10^{-4} K^{-1}, respectively. [35]

3.6. Refractive index

The refractive index values (n_D) of the studied ILs in the temperature range from (293.15 to 333.15) K at atmospheric pressure are shown in Table 4. The refractive indies of the ILs at 298.15 K varies from 1.5391 to 1.5682 with the lowest and the highest values correspond to [Bmim][SCN] and [C_2CNHeim][SCN], respectively. All the ILs have comparable refractive indexes with that of high-refraction material such as quartz crystal (n_D = 1.54) and liquid immersion oil (n_D = 1.51) [36]. This suggests that the ILs could be used as new optical materials. The refractive indexes of the current ILs are also high compared to their corresponding chloride based ILs. The refractive indexes of [C_2CNBim]Cl, [C_2CNAim]Cl and [C_2CNHeim]Cl at 298.15 K are 1.5243, 1.5460 and 1.5484. [24] For [C_2CNBim][SCN], [C_2CNAim][SCN] and [C_2CNHeim][SCN] the refractive indexes increased to 1.5483, 1.5563 and 1.5682. Moreover, the refractive index for [Bmim][SCN] at 298,15 K (n_D =1.5391) is higher than its counterpart ILs with $[NTf_2]^-$ (n_D =1.3880) [36], $[PF_6]^-$ (n_D = 1.4095), $[BF_4]^-$ (n_D = 1.4218), $[MeSO_4]^-$ (n_D = 1.4792), and [CF_3SO_3] (n_D = 1.4368). [37]

The refractive index increases in the order of [C_2CNHeim][SCN] > [C_2CNBzim][SCN] > [C_2CNAim][SCN] > [C_2CNBim][SCN] > [Bmim][SCN]. Deetlefs et al. [38] reported that refractive indexes decreases with increasing the molar volume for ILs with 1-alkyl-3-methylimidazolium homologous series. However, there is no direct relation between the molar volume and the refractive indexes for the present ILs. This could be because the ILs do not belong to the same homologous series as they contain different functional groups in the

imidazolium alkyl side-chain. The refractive index of the ILs depends on the nature of the functional groups incorporated in the imidazolium alkyl side-chain. The high refractive indexes of the nitrile, allyl, benzyl and hydroxyl functionalized ILs may be due to additional electron mobility around the nitrile, allyl, benzyl and hydroxyl functionalised side chain compared to the non-functionalized imidazolium alkyl chain.[23] This will be described latter using the DFT calculations.

Table 4. Experimental refractive index data as function of temperature at atmospheric pressure[a]

T/K	[Bmim] [SCN]	[C_2CNBim] [SCN]	[C_2CNAim] [SCN]	[C_2CNBzim] [SCN]	[C_2CNHeim] [SCN]
293.15	1.5406	1.5497	1.5578	1.5681	1.5692
298.15	1.5391	1.5483	1.5563	1.5666	1.5682
303.15	1.5375	1.5467	1.5548	1.5650	1.5666
308.15	1.5361	1.5453	1.5532	1.5634	1.5650
313.15	1.5346	1.5438	1.5517	1.5617	1.5640
318.15	1.5330	1.5424	1.5502	1.5602	1.5622
323.15	1.5316	1.5409	1.5488	1.5586	1.5605
328.15	1.5302	1.5396	1.5473	1.5571	1.5588
333.15	1.5286	1.5381	1.5458	1.5556	1.5572

[a]*Standard uncertainties u are u(T) = ± 0.05 K, and u(n_D) = ± 5×10^{-4}.*

Figure 3 shows the temperature dependences of the refractive indexes of the ILs. A linear relationship with temperature was obtained for all the ILs. The temperature dependences of the refractive indexes were correlated using linear equation. The correlation parameters, correlation coefficients and standard deviations are provided in supporting document (Table S4). The values of the correlation coefficients are greater than 0.99 while the maximum standard deviation less than 0.001 for all the studied ILs.

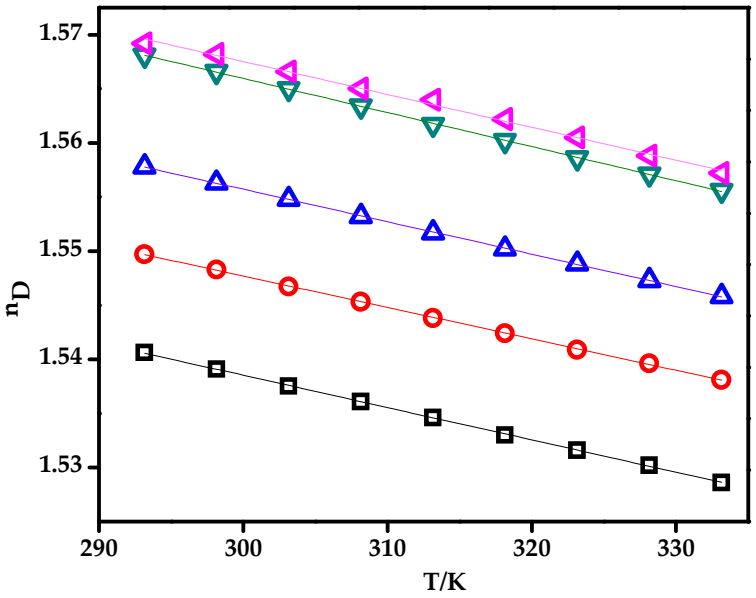

Figure 3. Temperature dependence of refractive indexes for the ILs. □, [Bmim][SCN]; ○, [C_2CNBim][SCN]; Δ, [C_2CNAim][SCN]; ∇, [C_2CNBzim][SCN]; ◁, [C_2CNHeim][SCN].

3.7. Density and refractive index correlations

Recently, the relationship between the refractive indexes and other physicochemical properties of ILs attracted much attention [37, 39]. In this work, the relation between density and refractive index of the ILs were correlated using various empirical equations which can be generally represented as:

$$f(n) = k\rho \tag{8}$$

where, f(n) is a function given by Lorentz-Lorenz, Dale-Gladstone, Newton, Eykman or modified Eykman equation, ρ density of the ILs and k the empirical constant that depends on the nature of ILs and the wavelength at which the refractive index is measured. The fitting parameters for equation (8) were obtained by correlating the experimental densities with refractive indexes of the ILs. The fitting parameter k for the various empirical equations and the constant for the modified Eykman equation are presented in Table 5**.** Among the empirical

equations the modified Eykman equation presents the best correlation between the present experimental densities and refractive indexes with an overall AAD % of 0.0047. Similar observations were reported by other Sorianoet and coworkers [37, 39]. This is because there are two parameters (*k* and *d*) in modified Eykman equation compared to only one mentioned in the other equations. The Eykman equation present less correlation for the densities and the refractive index with highest AAD which is 0.1966.

Table 5. Parameters *k* and *d* for different empirical equations from Equation (6)

		[Bmim][SCN]	[C_2CNBim][SCN]	[C_2CNAim][SCN]	[C_2CNBzim][SCN]	[C_2CNHeim][SCN]	AAD%
Lorentz-Lorenz[a]		0.2930	0.2842	0.2770	0.2784	0.2692	0.0544
Dale-Gladstone[b]		0.5035	0.4897	0.4785	0.4825	0.4667	0.0180
Eykman[c]		0.4632	0.4475	0.4348	0.4353	0.4205	0.1966
Newton[d]		1.2761	1.2457	1.2211	1.2361	1.1964	0.0708
Modified Eykman[e]	k	0.5787	0.4182	0.5971	0.5235	0.7405	0.0047
	d	0.6704	1.4350	0.5682	0.7995	0.0520	

$a\ f(n) = (n^2 - 1)/(n^2 + 2)$
$b\ f(n) = n - 1$
$c\ f(n) = (n^2 - 1)/(n^2 + 0.4)$
$d\ f(n) = n^2 - 1$
$e\ f(n) = (n^2 - 1)/(n + d)$

3.8. Viscosity

The dynamic viscosities of [Bmim][SCN] were compared with literatures data. [22, 40] The measurements and literatures data along with the deviations are included in supporting information (Table S5). The relative deviation between our measurement and the values reported by Vakili-Nezhaad et al. [22] varies from (0.48 to 7.86)% while the deviations from Domańska et al. [40] data are in the range of (0.10 to 0.75)%. Relatively higher discrepancies were observed between our measurement and that reported by Vakili-Nezhaad et al. [22] which could be due to the usage of different apparatus for the measurements.

Table 6. Dynamic viscosity (mPa.s) of ILs at various temperatures (298.15-353.15) K at atmospheric pressure[a]

T/K	[Bmim][SCN]	[C_2CNBim][SCN]	[C_2CNAim][SCN]	[C_2CNBzim][SCN]	[C_2CNHeim][SCN]
298.15	52.13	261.33	936.17	2219.95	1409.81
303.15	42.09	187.29	644.00	1304.93	887.67
308.15	35.04	137.95	419.54	788.15	555.56
313.15	29.21	104.68	279.8	489.12	363.03
318.15	24.31	81.5	199.08	311.89	244.39
323.15	20.73	64.59	145.54	195.73	168.16
328.15	16.78	51.77	108.64	145.36	118.44
333.15	15.02	41.94	82.48	98.61	84.24
338.15	12.79	34.63	64.13	65.35	62.22
343.15	11.09	29.47	51.65	48.63	47.47
348.15	9.97	25.64	42.74	36.13	37.29
353.15	8.32	21.38	33.94	29.38	28.33

[a]*Standard uncertainties u are u(T) = ± 0.01 K and viscosity u(η) =* ± 0.32%.

The dynamic viscosities of the ILs in temperature range of (298.15-353.15) K are shown in Table 6. The viscosity values are in the order of [Bmim][SCN] < [C_2CNBim][SCN] < [C_2CNAim][SCN] < [C_2CNHeim][SCN] < [C_2CNBzim][SCN]. The same trend was observed for chloride based ILs with similar cations, that is, [C_2CNBim]Cl < [C_2CNAim]Cl < [C_2CNHeim]Cl < [C_2CNBzim]Cl. [24] The viscosities of the non-functionalized [Bmim][SCN] is much lower than ILs functionalized with nitrile, allyl, benzyl and hydroxyl groups. For example, when the methyl group of [Bmim][SCN] is replaced by propyronitrile (CH_2-CH_2-CN) in [C_2CNBim][SCN], the dynamic viscosity at 298.15 K increases from 52.13 to 261.33 mPa.s. The result is consistent with the result reported by Zhang et al. [23], where the viscosity increases from 44 to 286 mPa.s when the butyl of [Bmim][NTf_2] is replaced by CH_2-CH_2-CN. Moreover, the dual functionalized ILs have higher viscosity compared to the mono-functionalized [C_2CNBim][SCN]. This can be explained by comparing the viscosity of [C_2CNBim][SCN] with

[C_2CNAim][SCN], [C_2CNBzim][SCN] and [C_2CNHeim][SCN]. For dual functionalized ILs, the viscosity increases in the order of [C_2CNBim][SCN] < [C_2CNAim][SCN] < [C_2CNHeim][SCN] < [C_2CNBzim[SCN]. The increased hydrogen bonding interactions, π-π stacking and electrostatic interactions derived from the functional groups may be responsible for the increases in the viscosity of the functionalized ILs. Similar trend was observed for their counterpart ILs with chloride anion. [24]

Figure 4 shows the effect of temperature on viscosities of the ILs. The temperature has a profound effect on the viscosity, and the viscosity is particularly more affected at lower temperature, that is, the viscosity decreases sharply with increasing temperature at lower temperature. The dynamic viscosities η were fitted as a function of temperature using the following equation: [22]

$$\ln(\eta/mPa.s) = C_0 + C_1/T + C_2/T^2 \quad (9)$$

where, η is the dynamic viscosity, T is the temperature, and C_0 C_1 and C_2 are the adjustable parameters. The fitting parameters are provided in supporting information (Table S6). The equation correlates the experimental dynamic viscosity in the experimental temperature ranges with reasonable accuracy as shown in Figure 4. It can be concluded that the equations correlated successfully the experimental data with $R^2 > 0.99$ and maximum standard deviation of 0.0301.

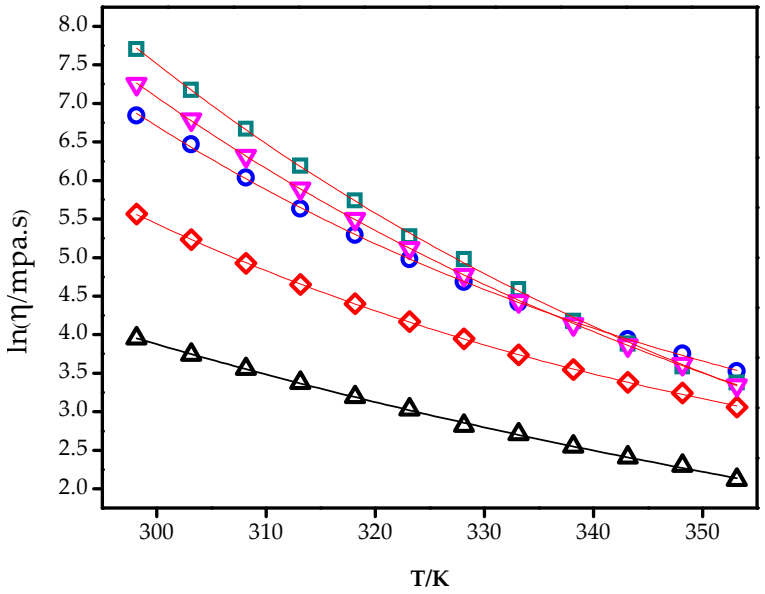

Figure 4. Viscosity of ILs as function of temperature. Δ, [Bmim][SCN]; ◊, [C_2CNBim][SCN]; ○, [C_2CNAim][SCN]; ∇, [C_2CNBzim][SCN]; □, [C_2CNHeim][SCN].

3.9. Thermal Stability

Due to their negligible vapour pressure and high chemical stability, ILs have been proposed for many high temperature applications. For safe application at elevated temperature, it is important to test the behaviour of the ILs at the operating conditions, and determine their maximum operation temperatures. TGA is the most commonly used technique to investigate the short-term thermal stability, also known as dynamic analysis. In TGA analysis, the thermal stabilities are usually reported in terms of onset temperature (T_{onset}), which is the cross point between the tangent straight lines to the TGA curve before and after decomposition started. However, since thermal degradation usually starts at a lower temperature, known as starting temperature (T_{start}), the T_{onset} may not represent the maximum operation temperature of the ILs. That means, the T_{onset} could overestimated the maximum operation temperature. Moreover, some authors also reported the thermal behaviour of ILs in terms of $T_{10\%}$ [21] and T_{peak}. [41] The $T_{10\%}$ is the temperature at which 10 wt % of the mass degrade while T_{peak} is the temperature at which maximum degradation

observed. The T_{peak} is obtained from derivative thermogravimetric curve. In this work, T_{start}, T_{onset}, $T_{10\%}$ and T_{peak} were reported to characterize the thermal stability of the ILs.

Table 7. Dynamic TGA characteristic parameters (T_{start}, T_{onset}, $T_{10\%}$ and T_{peak}) of the ILs.

T/K	[Bmim] [SCN]	[C_2CNBim] [SCN]	[C_2CNAim] [SCN]	[C_2CNBzim] [SCN]	[C_2CNHeim] [SCN]
T_{start}	496	480	470	479	465
$T_{10\%}$	524	510	500	507	499
T_{onset}	536	509	504	507	485
T_{peak}	546	553	540	549	548

The dynamic thermal decomposition characteristic parameters (T_{start} T_{onset}, $T_{10\%}$ and T_{peak}) of the ILs are shown in Table 7. The thermogravimetric traces are included in the supporting information (Figure S2). For a given ILs, the T_{start}, T_{onset}, and T_{peak} follow the order of $T_{start} < T_{onset} < T_{peak}$ which present that the ILs start decomposition before the onset temperature and the maximum decompositions occur after the onset temperature is observed. The difference between the T_{onset} and T_{start} varies from 20 K for [C_2CNHeim][SCN] to 40 K for [Bmim][SCN]. Similarly, the difference between T_{peak} and T_{onset} varies from (10 to 63) K for the studied ILs. The lowest and the highest differences are for observed for [Bmim][SCN] and [C_2CNHeim][SCN], respectively.

Introduction of the functional groups reduces the thermal stabilities of the ILs. The result is in agreement with previous observation on the effect functionalized cation on thermal stability of the ILs [41-44]. Gao and Mu [41] reported that replacing the saturated alkyl chain with unsaturated side alkyl chain generally decreases the thermal decomposition of the ILs irrespective of the nature of the anions. They also explained the low thermal stability of allyl functionalized ILs may be due to the rigidity of the allyl group. Hao et al. [42] related the low thermal stability of ally functionalized ILs to their low activation energy compared to ILs without allyl functional group.

Similarly, introducing hydroxyl functional group in the imidazolium alkyl side-chain decreases the thermal stabilities of the ILs. This could be due to the higher chemical activity and easier decomposition of the hydroxyethyl functional group [44].

3.10. Computational study

Density functional theory (DFT) calculations were carried out to understand the effect of the functional groups in imidazolium alkyl side-chain on the molecular properties of the ILs. First, the structures of the cations were optimized and stable conformers were obtained. Then, ions pairs, each consists one of the cations and thiocyanate anion, were optimized to obtain the ILs. The most stable structures of the cations and the ILs (ions pairs) are included in supporting information (Figure S3). The electronic structure of imidazolium ring contains delocalized 3-centered-4-electron configuration across the N_1-C_2-N_3 moiety, a double bond between C_4 and C_5 and a weak delocalization in the central region [45] (Figure 5 (a)). Although the hydrogen atoms on C_2-H, C_4-H, and C_5-H carry positive charges, the C_2-H is more acidic since it is located between two electronegative nitrogen atoms. This could also be observed from the COSMO-surface charge density obtained from the quantum calculations.

Figure 5 shows the structure of $[Bmim]^+$ with its COSMO-surface charge density. The blue surface shows the positive charges due to acidic hydrogen from C_2-H, C_4-H and C_5-H of the imidazolium ring. Since C_2-H is more acidic than C_4-H and C_5-H the thiocyanate anion preferably interacts with the C_2-H side of the imidazolium ring. Thus, most stable cation-anion pair was obtained when thiocyanate anion is placed near to the C_2-H as shown in Figure 5 (c). However, for the nitrile, allyl, benzyl and hydroxyl functionalized cations/ILs their electronic structural properties are also affected by the functional group incorporated in the imidazolium alkyl side-chain. This can be observed from the COSMO-surface charge of $[C_2CNHeim]^+$ shown

in Figure 5 (c), which is contains both nitrile and hydroxyl functional groups. The nitrile functional group introduces electron deficient region on the C_2CN part of the alkyl spacer while the hydroxyl group introduces both electron deficient (acidic) and excess electron (basic) regions. This shows $[C_2CNHeim]^+$ could interact with the thiocyanate anions through the acid hydrogen from the hydroxyl functional in addition to the C_2-H of imidazolium ring. The stable structures and COSMO-charge distribution of all the studied cations and ILs are included in supporting document (Figure S3).

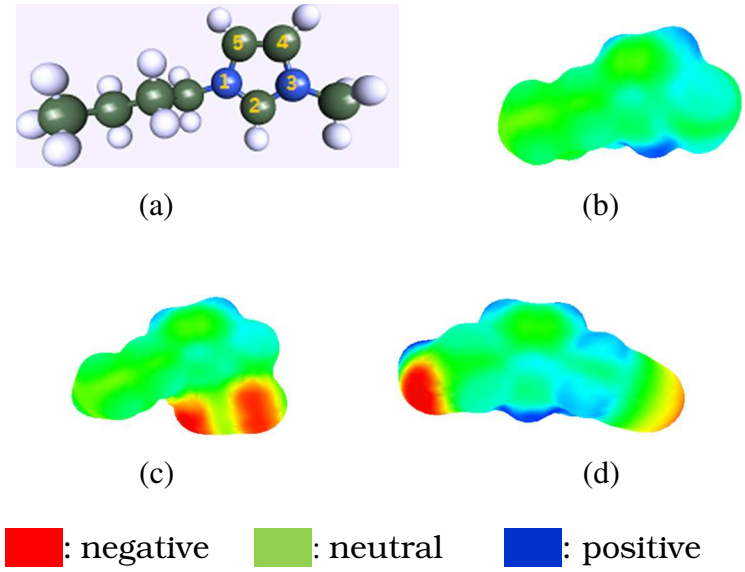

Figure 5. Optimized structure and COSMO-surface charge distributions. (a) $[Bmim]^+$ structure; (b) $[Bmim]^+$ COSMO-surface charge distributions; (c) [Bmim][SCN] COSMO-surface charge distributions; (d) $[C_2CNHeim]^+$ COSMO-surface charge distributions.

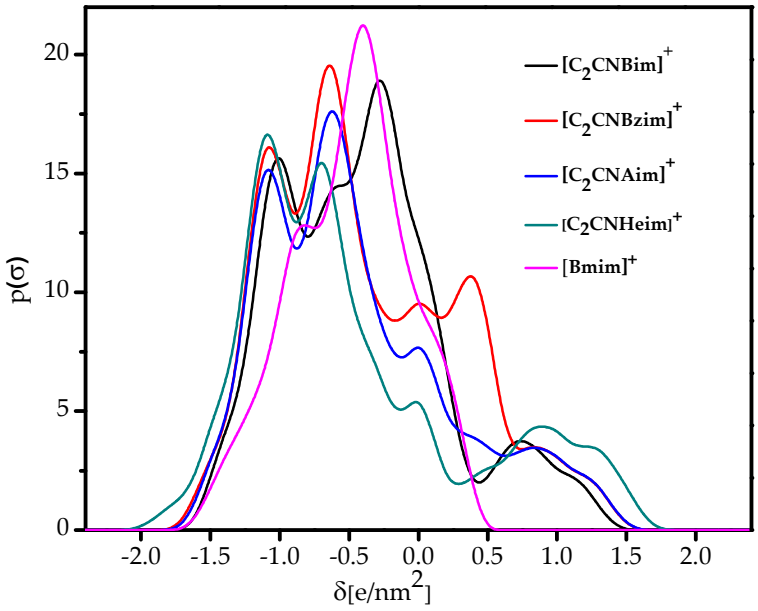

Figure 6. Sigma-profile of the studied cation computed by COSMO-RS

The effect of the functional groups on the electronic properties of the ILs can also be observed from the sigma-profile (σ-profile) of the ILs. The σ-profile shows the screening charge densities which is expressed in term of relative amount of surface with polarity σ for a given molecule. Figure 6 shows the σ-profile of the studied cations. The σ-profile of $[Bmim]^+$ extends from (-1.7 to 0.8) e/nm^2 with maximum peak at about -0.4 e/nm^2 while for functionalized cations the σ-profile has wider ranges. For example, the σ-profile of $[C_2CNHeim]^+$ is in the range of (-2.0 to 1.8) e/nm^2. If the a molecule or ionic species has σ-profile peaks in the range of $\sigma > 1.0$ or/ and $\sigma < 1.0$, it will have hydrogen bond donor or/and acceptor property. [30] $[C_2CNHeim]^+$ has more extended σ-profile which indicates its strong hydrogen bond donor and acceptor capacity as mentioned in the previous sections.

To understand how the cations could interact with thiocyanate anion the Highest Occupied Molecular Orbital (HOMO) and Lowest Occupied Molecular Orbital (LUMO) were retrieved from Natural Bond Orbital (NBO) analysis. The HOMO and LUMO analyses can give insight into the chelating process of cation-anion systems. LUMO is associated with the tendency of a

species to receive electron and is characteristic for electrophilic components while HOMO is associated with the tendency to donate electron and is characteristic for nucleophilic components. [46] Thus, the HOMO and LUMO are a likely location for a bond to occur between the cations and the thiocyanate anion because the incommoding electron from HOMO of one molecule will fill into the LUMO of another molecule.

Figure 7 shows the HOMO and LUMO orbitals of some of the cations and ILs studied. The full data are provided in supporting information (Figure S4). For $[Bmim]^+$ the LOMO orbitals localized at N_1-C_2-N_3 of the imidazolium ring while the HOMO part distributed on the π-system on top and lower part of the imidazolium ring (Figure 7 (a) and (b)). Since anions are generally the source of HOMO orbitals in cation-anion interaction, the anions transfer electrons to the LUMO of the cation, that is, cation-anion interaction is preferably occurs through HOMO of thiocyanate anion and LUMO of $[Bmim]^+$ cation. On the contrary, for functionalized imidazolium based cations HOMO does not limited to the imidazolium π-system but also contributed by the functional groups. For example, for $[C_2CNBim]^+$ the source of HOMO is both the π-system and the nitrile functional group in the alkyl side-chain (Figure 7 (c) and (d)). For dual functionalized cations $[C_2CNAim]^+$, $[C_2CNBzim]^+$ and $[C_2CNHeim]^+$ the allyl, benzyl and hydroxyl functional groups contributed to the HOMO orbitals. Moreover, in the case of $[C_2CNHeim]^+$ the hydroxyl functional group is also a source of LUMO orbitals because of its both hydrogen bond donor and acceptor behaviour (Figure 7 (e) and (f)). These could affect the cation-anion interaction which consecutively determines the properties of the ILs.

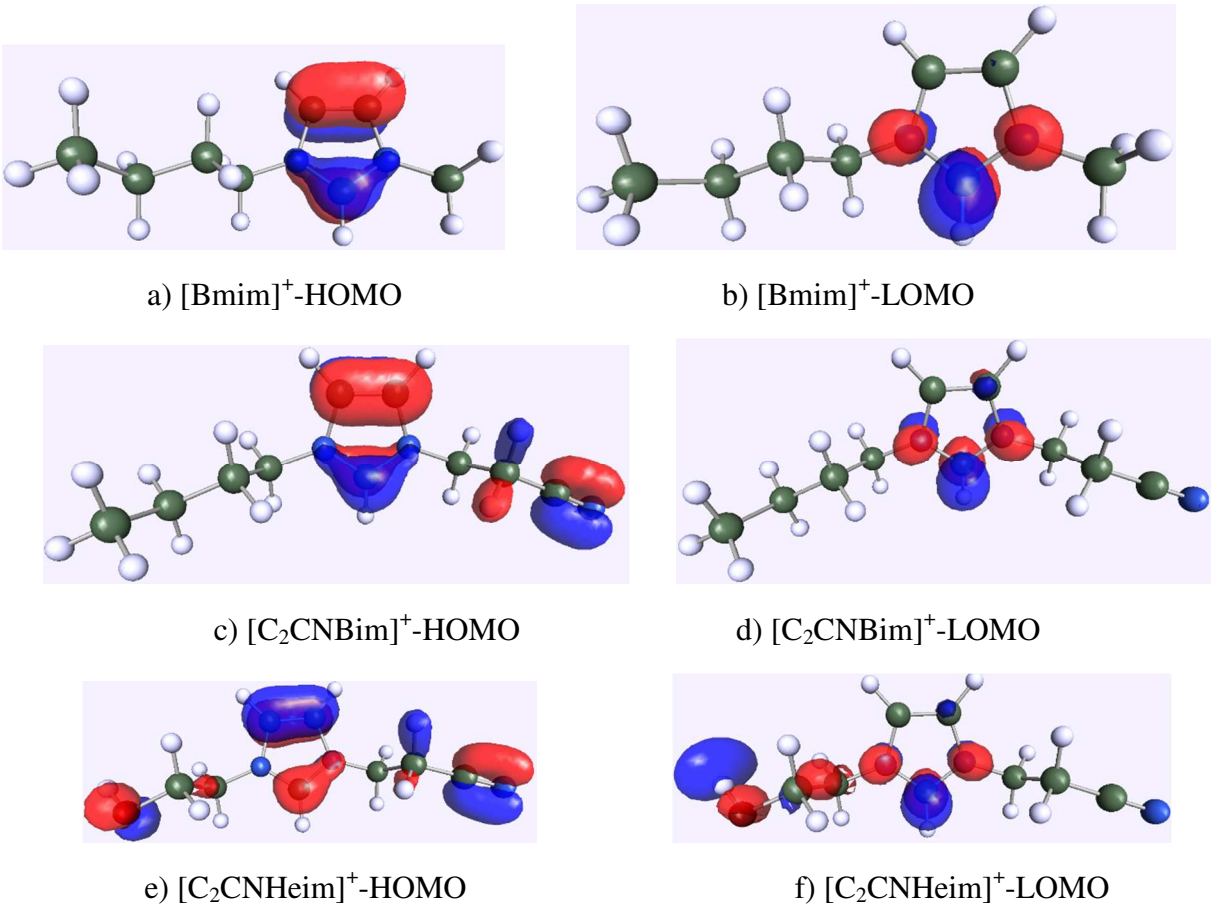

a) [Bmim]$^+$-HOMO b) [Bmim]$^+$-LOMO

c) [C_2CNBim]$^+$-HOMO d) [C_2CNBim]$^+$-LOMO

e) [C_2CNHeim]$^+$-HOMO f) [C_2CNHeim]$^+$-LOMO

Figure 7. HOMO and LUMO orbitals of studied cations.

The properties of the ILs are not only determined by the cation-anion interaction but also by intermolecular interactions between the ILs molecules. To see the interactions between ILs the HOMO and LUMO of the ILs were generated for the ILs. Figure 8 shows the HOMO and LUMO of selected ILs. Full data on HOMO and LUMO all the studied ILs can be found in supporting information (Figure S5). For [Bmim][SCN], the HOMO orbitals mainly comes from the thiocyanate while the LOMO is located on N_1-C_2-N_3 of the imidazolium ring. However, in the case of [C_2CNBim][SCN], nitrile functional group is also the source of HOMO and could contribute to the intermolecular interaction. For dual functionalized ILs [C_2CNAim][SCN], [C_2CNBzim] [SCN], and [C_2CNHeim] [SCN] the allyl, benzyl and hydroxyl functional groups

contributed to strong between the ILs molecules since they are the source HOMO or LUMO orbitals.

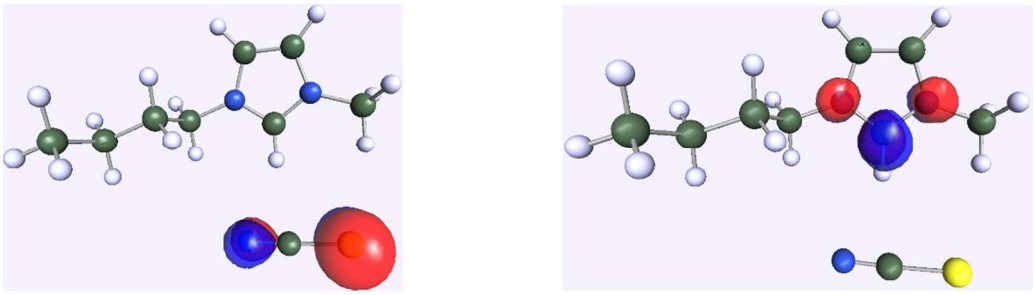

a) [Bmim][SCN]-HOMO b)[Bmim][SCN]-LUMO

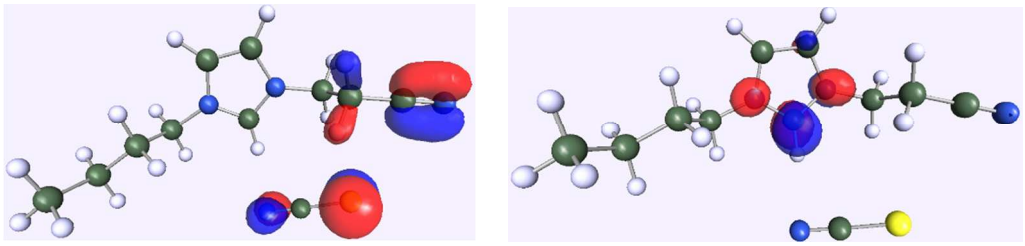

c) [C_2CNBim][SCN]-HOMO d) [C_2CNBim][SCN]-LOMO

Figure 8. HOMO and LUMO orbitals of studied ILs.

4. CONCLUSIONS

Nitrile containing side chain was added to the imidazole ring through Michael addition reaction followed by addition of each allyl, benzyl, and hydroxyl ethyl functional groups to synthesize their respective ILs. The effects of the functional groups on some of their thermophysical properties were studied. The measured density values are in the order of [Bmim][SCN] < [C_2CNBim][SCN] < [C_2CNAim][SCN] < [C_2CNBzim][SCN] < [C_2CNHeim][SCN]. The incorporation of nitrile functionality in the imidazolium alkyl side-chain increases the density of the ILs by more than 4% subsequent addition of allyl, benzyl and hydroxyl in other side of the cation increases by 8%, 9% and 12 %, respectively. The refractive indexes of the ILs increases in

the order of [Bmim][SCN] < [C_2CNBim][SCN] < [C_2CNAim][SCN] < [C_2CNBzim][SCN] < [C_2CNHeim][SCN]. The density and refractive index values are best correlated with Eykman empirical equation. Incorporation of the functional groups increases the viscosity of the ILs. The dynamic viscosities also increases in the order of [Bmim][SCN] < [C_2CNBim][SCN] < [C_2CNAim][SCN] < [C_2CNBzim][SCN] < [C_2CNHeim][SCN]. However, the ILs containing the functional groups in their imidazolium alkyl spacer have lower thermal stability. The density functions theory (DFT) calculations show that the incorporation of the functional groups in the imidazolium alky chain creates more electron deficient and/or electron excess regions. This could affect the cation-anion interactions and also interactions between the ILs molecules which thereby affects their properties.

AUTHOR INFORMATION

Corresponding Author

*Tel.: (60) 175667304. E-mail: kiyaagonfaa@gmail.com.

ACKNOWLEDGEMENTS

This work is supported by fundamental research grant scheme (ERGS-0153AB-110) of Ministry of Higher Education of Malaysia and Universiti Teknologi PETRONAS.

ASSOCIATED CONTENT

Supporting Information

Experimental and literature density and viscosity of for 1-butyl-3-methylimidazolium thiocyanate (Table S1 and S5). Correlation parameters for density, refractive index and viscosity as function of temperature (Table S2, S4 and S6). Isobaric thermal expansion coefficient of the ILs (Table S3). Comparison of experimental and literature densities of 1-butyl-3-

methylimidazolium thiocyanate (Figure S1). TGA of ionic liquids (Table S2). Optimized structure and sigma charge distribution and HOMO-LUMO orbitals (Figure S3-S5).

REFERENCES

1. Meindersma, G. W.; De Haan, A. B., Cyano-containing ionic liquids for the extraction of aromatic hydrocarbons from an aromatic/aliphatic mixture. *Science China Chemistry* **2012,** 55, (8), 1488-1499.

2. MacFarlane, D. R.; Golding, J.; Forsyth, S.; Forsyth, M.; Deacon, G. B., Low viscosity ionic liquids based on organic salts of the dicyanamide anion. *Chemical communications* **2001**, (16), 1430-1431.

3. Yoshida, Y.; Baba, O.; Saito, G., Ionic liquids based on dicyanamide anion: Influence of structural variations in cationic structures on ionic conductivity. *The Journal of Physical Chemistry B* **2007,** 111, (18), 4742-4749.

4. Yoshida, Y.; Muroi, K.; Otsuka, A.; Saito, G.; Takahashi, M.; Yoko, T., 1-Ethyl-3-methylimidazolium based ionic liquids containing cyano groups: synthesis, characterization, and crystal structure. *Inorganic chemistry* **2004,** 43, (4), 1458-1462.

5. Yoshida, Y.; Fujii, J.; Muroi, K.; Otsuka, A.; Saito, G.; Takahashi, M.; Yoko, T., Highly conducting ionic liquids based on l-ethyl-3-methylimidazolium cation. *Synthetic metals* **2005,** 153, (1), 421-424.

6. Deng, M.-J.; Chen, P.-Y.; Leong, T.-I.; Sun, I.-W.; Chang, J.-K.; Tsai, W.-T., Dicyanamide anion based ionic liquids for electrodeposition of metals. *Electrochemistry Communications* **2008,** 10, (2), 213-216.

7. Zhou, D.; Bai, Y.; Zhang, J.; Cai, N.; Su, M.; Wang, Y.; Zhang, M.; Wang, P., Anion effects in organic dye-sensitized mesoscopic solar cells with ionic liquid electrolytes: tetracyanoborate vs dicyanamide. *The Journal of Physical Chemistry C* **2010,** 115, (3), 816-822.

8. Marszalek, M.; Fei, Z.; Zhu, D.-R.; Scopelliti, R.; Dyson, P. J.; Zakeeruddin, S. M.; Grätzel, M., Application of ionic liquids containing tricyanomethanide $[C(CN)_3]^-$ or tetracyanoborate $[B(CN)_4]^-$ anions in dye-sensitized solar cells. *Inorganic chemistry* **2011,** 50, (22), 11561-11567.

9. Bustam, M. A.; Muhamad, A. H.; Gonfa, G.; Man, Z., Benzene and Cyclohexane Separation Using 1-propanenitrile-3-butylimidazolium dicyanamide ionic liquid. *Advanced Materials Research* **2014,** 879, 58-62.

10. Gonfa, G.; Bustam, M. A.; Murugesan, T.; Man, Z.; Mutalib, M. A., Thiocyanate Based Task-specific Ionic Liquids for Separation of Benzene and Cyclohexane. *Chemical Engineering* **2013,** 32.

11. Cui, G.; Zhang, F.; Zhou, X.; Li, H.; Wang, J.; Wang, C., Tuning the Basicity of Cyano-Containing Ionic Liquids to Improve SO_2 Capture through Cyano–Sulfur Interactions. *Chemistry-A European Journal* **2015,** 21, (14), 5632-5639.

12. Cláudio, A. F. M.; Freire, M. G.; Freire, C. S.; Silvestre, A. J.; Coutinho, J. A., Extraction of vanillin using ionic-liquid-based aqueous two-phase systems. *Separation and Purification Technology* **2010,** 75, (1), 39-47.

13. Muhammad, N.; Man, Z.; Bustam, M. A.; Mutalib, M. A.; Rafiq, S., Investigations of novel nitrile-based ionic liquids as pre-treatment solvent for extraction of lignin from bamboo biomass. *Journal of Industrial and Engineering Chemistry* **2013,** 19, (1), 207-214.

14. Domańska, U.; Królikowska, M.; Królikowski, M., Phase behaviour and physico-chemical properties of the binary systems {1-ethyl-3-methylimidazolium thiocyanate, or 1-ethyl-3-methylimidazolium tosylate+ water, or+ an alcohol}. *Fluid Phase Equilibria* **2010,** 294, (1), 72-83.

15. Klomfar, J.; Součková, M.; Pátek, J., Temperature dependence of the surface tension and density at 0.1 MPa for 1-ethyl-and 1-butyl-3-methylimidazolium dicyanamide. *Journal of Chemical & Engineering Data* **2011,** 56, (8), 3454-3462.

16. Sánchez, L. G.; Espel, J. R.; Onink, F.; Meindersma, G. W.; Haan, A. B. d., Density, viscosity, and surface tension of synthesis grade imidazolium, pyridinium, and pyrrolidinium based room temperature ionic liquids. *Journal of Chemical & Engineering Data* **2009,** 54, (10), 2803-2812.

17. Tong, J.; Liu, Q.-S.; Kong, Y.-X.; Fang, D.-W.; Welz-Biermann, U.; Yang, J.-Z., Physicochemical properties of an ionic liquid $[C_2mim][B(CN)_4]$. *Journal of Chemical & Engineering Data* **2010,** 55, (9), 3693-3696.

18. Królikowska, M.; Hofman, T., Densities, isobaric expansivities and isothermal compressibilities of the thiocyanate-based ionic liquids at temperatures (298.15–338.15 K) and pressures up to 10MPa. *Thermochimica Acta* **2012,** 530, 1-6.

19. Quijada-Maldonado, E.; Van der Boogaart, S.; Lijbers, J.; Meindersma, G.; De Haan, A., Experimental densities, dynamic viscosities and surface tensions of the ionic liquids series 1-ethyl-3-methylimidazolium acetate and dicyanamide and their binary and ternary mixtures with water and ethanol at T =(298.15 to 343.15 K). *The Journal of Chemical Thermodynamics* **2012,** 51, 51-58.

20. Kamal, A.; Chouhan, G., A task-specific ionic liquid [bmim] SCN for the conversion of alkyl halides to alkyl thiocyanates at room temperature. *Tetrahedron letters* **2005,** 46, (9), 1489-1491.

21. Navarro, P.; Larriba, M.; Rojo, E.; García, J. n.; Rodríguez, F., Thermal properties of cyano-based ionic liquids. *Journal of Chemical & Engineering Data* **2013,** 58, (8), 2187-2193.

22. Vakili-Nezhaad, G.; Vatani, M.; Asghari, M.; Ashour, I., Effect of temperature on the physical properties of 1-butyl-3-methylimidazolium based ionic liquids with thiocyanate and tetrafluoroborate anions, and 1-hexyl-3-methylimidazolium with tetrafluoroborate and hexafluorophosphate anions. *The Journal of Chemical Thermodynamics* **2012,** 54, 148-154.

23. Zhang, Q.; Li, Z.; Zhang, J.; Zhang, S.; Zhu, L.; Yang, J.; Zhang, X.; Deng, Y., Physicochemical properties of nitrile-functionalized ionic liquids. *The Journal of Physical Chemistry B* **2007,** 111, (11), 2864-2872.

24. Muhammad, N.; Man, Z.; Ziyada, A. K.; Bustam, M. A.; Mutalib, M. A.; Wilfred, C. D.; Rafiq, S.; Tan, I. M., Thermophysical properties of dual functionalized imidazolium-based ionic liquids. *Journal of Chemical & Engineering Data* **2012,** 57, (3), 737-743.

25. Turbomole 6.2 (http://www.turbomole-gmbh.com/turbomole-manuals/45-turbomole-62-manual.html (accessed 25.08.15). In.

26. Perdew, J. P., Density-functional approximation for the correlation energy of the inhomogeneous electron gas. *Physical Review B* **1986,** 33, (12), 8822.

27. Becke, A. D., Density-functional exchange-energy approximation with correct asymptotic behavior. *Physical Review A* **1988,** 38, (6), 3098.

28. Eichkorn, K.; Weigend, F.; Treutler, O.; Ahlrichs, R., Auxiliary basis sets for main row atoms and transition metals and their use to approximate Coulomb potentials. *Theoretical Chemistry Accounts* **1997,** 97, (1-4), 119-124.

29. Schäfer, A.; Huber, C.; Ahlrichs, R., Fully optimized contracted Gaussian basis sets of triple zeta valence quality for atoms Li to Kr. *The Journal of Chemical Physics* **1994,** 100, (8), 5829-5835.

30. COSMOtherm Users Manual (Version C2.1) http://www.cosmologic.de/support-download/manuals-documentation.html.

31. Zhang, S.; Qi, X.; Ma, X.; Lu, L.; Zhang, Q.; Deng, Y., Investigation of cation-anion interaction in 1-(2-hydroxyethyl)-3-methylimidazolium based ion pairs by density functional theory calculations and experiments. *Journal of Physical Organic Chemistry* **2011,** 25, (3), 248-257.

32. Hu, Y.; Peng, X., Effect of the Structures of Ionic Liquids on Their Physical Chemical Properties. In *Structures and Interactions of Ionic Liquids*, Springer: 2014; pp 141-174.

33. Glasser, L., Lattice and phase transition thermodynamics of ionic liquids. *Thermochimica acta* **2004,** 421, (1), 87-93.

34. Lide, D. R., *CRC handbook of chemistry and physics*. CRC press: 2004.

35. Gu, Z.; Brennecke, J. F., Volume expansivities and isothermal compressibilities of imidazolium and pyridinium-based ionic liquids. *Journal of Chemical & Engineering Data* **2002,** 47, (2), 339-345.

36. Seki, S.; Tsuzuki, S.; Hayamizu, K.; Umebayashi, Y.; Serizawa, N.; Takei, K.; Miyashiro, H., Comprehensive refractive index property for room-temperature ionic liquids. *Journal of Chemical & Engineering Data* **2012,** 57, (8), 2211-2216.

37. Soriano, A. N.; Doma Jr, B. T.; Li, M.-H., Measurements of the density and refractive index for 1-n-butyl-3-methylimidazolium-based ionic liquids. *The Journal of Chemical Thermodynamics* **2009,** 41, (3), 301-307.

38. Deetlefs, M.; Seddon, K. R.; Shara, M., Predicting physical properties of ionic liquids. *Physical Chemistry Chemical Physics* **2006,** 8, (5), 642-649.

39. Soriano, A. N.; Doma Jr, B. T.; Li, M.-H., Density and refractive index measurements of 1-ethyl-3-methylimidazolium-based ionic liquids. *Journal of the Taiwan Institute of Chemical Engineers* **2010,** 41, (1), 115-121.

40. Domańska, U.; Królikowska, M., Density and Viscosity of Binary Mixtures of {1-Butyl-3-methylimidazolium Thiocyanate + 1-Heptanol, 1-Octanol, 1-Nonanol, or 1-Decanol}. *Journal of Chemical & Engineering Data* **2010,** 55, (9), 2994-3004.

41. Cao, Y.; Mu, T., Comprehensive Investigation on the Thermal Stability of 66 Ionic Liquids by Thermogravimetric Analysis. *Industrial & engineering chemistry research* **2014,** 53, (20), 8651-8664.

42. Hao, Y.; Peng, J.; Hu, S.; Li, J.; Zhai, M., Thermal decomposition of allyl-imidazolium-based ionic liquid studied by TGA–MS analysis and DFT calculations. *Thermochimica Acta* **2010,** 501, (1), 78-83.

43. Maton, C.; De Vos, N.; Stevens, C. V., Ionic liquid thermal stabilities: Decomposition mechanisms and analysis tools. *Chemical Society Reviews* **2013,** 42, (13), 5963-5977.

44. Song, Y.; Xia, Y.; Liu, Z., Influence of cation structure on physicochemical and antiwear properties of hydroxyl-functionalized imidazolium bis (trifluoromethylsulfonyl) imide ionic liquids. *Tribology Transactions* **2012,** 55, (6), 738-746.

45. Bustam, M.; Gonfa, G.; Man, Z.; Abdul Mutalib, M., Unique Structure and Solute–Solvent Interaction in Imidazolium based Ionic Liquids. *Research Journal of Chemistry and Environment* **2012,** 16, (1), 93-103.

46. Shahid, R.; Muhammad, N.; Gonfa, G.; Toprak, M. S.; Muhammed, M., Synthesis, COSMO-RS analysis and optical properties of surface modified ZnS quantum dots using ionic liquids. *Journal of Physics and Chemistry of Solids* **2015,** 85, 34-38.